

MOŽNOST MERJENJA DINAMIČNEGA ODZIVA KONSTRUKCIJ Z NEKONTAKTNO GEODETSKO METODO

THE POSSIBILITY OF MEASURING THE DYNAMIC RESPONSE OF STRUCTURES USING NON-CONTACT GEODETTIC METHOD

Boštjan Kovačič, Tomaž Motob

UDK: 528.48:624.07
Klasifikacija prispevka po COBISS.SI: 1.01
Prispelo: 3. 8. 2018
Sprejeto: 6. 1. 2019

DOI: 10.15292/geodetski-vestnik.2019.01.57-72
SCIENTIFIC ARTICLE
Received: 3. 8. 2018
Accepted: 6. 1. 2019

IZVLEČEK

Gradbene konstrukcije so podvržene različnim dejavnikom, katerih posledice je treba redno spremljati. To lahko izvedemo v obliki kontrolnih meritev ali opazovanj. Namen prispevka je prikazati uporabnost geodetskih nekontaktnih metod pri določanju dinamičnega odziva konstrukcij. Za simulacijo smo uporabili lamelo, na kateri smo z različnimi metodami spremljali dinamični odziv, poudarek pa je na sodobni geodetski metodi z uporabo robotskega elektronskega tahimera RTS (angl. Robotic Total Station). Za določitev dinamičnega odziva je podrobneje opisan algoritem za določanje srednje amplitude harmoničnega nihanja in metodi spektralne analize vzorčenih podatkov. Rezultati, dobljeni z metodo RTS, so pokazali visoko stopnjo zanesljivosti določitve dinamičnega odziva.

ABSTRACT

Building construction is the subject of various factors and their consequences must be regularly monitored; this can be carried out in the form of control measurements or monitoring. This article aims to show the usability of geodetic non-contact methods in defining the dynamic response of structures. The lamella on which various methods for monitoring the dynamic response was used for simulation; the emphasis is on a modern geodetic method using a Robotic Total Station (RTS). To determine the dynamic response, the algorithm for the determination of the harmonic oscillation's average amplitude and the methods of the spectral analysis of the sampled data is further described. The results obtained with the RTS method have shown a high level of reliability for the determination of dynamic response.

KLJUČNE BESEDE

geodezija, inženirska geodezija, gradbeništvo, dinamični odziv konstrukcij, robotski elektronski tahimeter

KEY WORDS

geodesy, engineering geodesy, civil engineering, dynamic response of the structure, robotic total station

1 INTRODUCTION

Information on actual response of a structure under loads is an important part of estimating the state and safety of structures in their exploitation period. When objects are exposed to dynamic traffic loads, it is necessary to know the objects' *behaviour* at cyclical errors. There are various methods for determining dynamic characteristics of objects; simultaneously with a development, there are more and more geodetic methods being used. Nowadays, geodetic instruments measure not only static or very slow displacements but also fast and, more importantly, dynamic ones. Determining actual deformations of building objects under the influence of dynamic loads has until recently been an unresolved problem from the point of geodesy. Systematic measurements of the displacements of more flexible building objects (bridges, high buildings) have begun to be carried out with the outbreak of advanced geodetic technologies and positioning systems, such as GNSS (Global Navigation Satellite System), which enabled to capture the sufficient number of measurements of a position in a certain time interval. The system works on the principle of connection with satellites, therefore, the condition to perform such measurements is to have an unobstructed view of the horizon and the presence of a sufficient number of satellites. The issues arise in narrow basins and ravines or in urban settlements where the visibility of the satellites during the whole duration of measurement is not likely to be granted. The accuracy to determine the position based on satellites observations depends especially on the geometrical layout of observed satellites and on the quality of performed observations. The quality of the performed observations, along with the quality of the receiver, depends also on the quality of the treatment of errors on the observations. The errors on the GNSS observations can be in general, considering their origin, divided onto errors with satellites, receiver or the media. Some mentioned errors are systematic, some of them not. In the procedure of the treatment of the observations, it is necessary to assess especially systematic errors of the GNSS observations. Systematic errors can be removed with the use of adequate mathematical models; they can be diminished or even removed with adequate combinations of observations or with adequately performed geodetic GNSS observations, including using Global Positioning System GPS (Kogoj, 2011).

Dynamic tests have recently become more and more widespread. They are regarded as the complete techniques for monitoring the bridging objects and they enable the global assessment of a structure (Palazzo, 2006). First studies and projects of determining displacements and deformations of structure objects with the assistance of geodetic measurements appeared in the 1990s (DeLoach, 1989). The first uses of GPS measurement systems to determine displacements and deformations of dams appeared toward the end of the 1980s (Rueger, 2006). Newer studies are directed towards the possibility to use geodetic measurement systems in the projects of dynamic monitoring of the objects. After the first projects of dynamic monitoring with the use of geodetic instruments, primary GPS, the studies have been directed towards the integration of sensors and operativity of the monitoring system. The experts have directed their work towards the integration of GPS and other sensors (accelerometers, pseudolites, etc.) to exploit the advantages and avoid the limits of individual systems. Researchers at the University of Tokyo in Japan and at the University of New South Wales in Australia have made a whole range of measurements on a 110 m high steel tower in Tokyo with a use of GPS technology, accelerometers and sensors with optical fibre and thus provided an answer on the response of a structure on earthquakes and hurricanes (Li, 2004a, 2004b, 2005, 2006). Researchers from the University of Nottingham in Great Britain have directed their research work into the integration of measuring devices GPS and accelerome-

ters at the monitoring projects of hanging bridges (Roberts, 1999, 2000, 2001, 2004; Meng, 2007). In association with researchers from the University of New South Wales in Australia, the research focused on methodology and integration of GPS measuring devices and pseudolites with the aim to improve the accuracy of positioning the height component, which is 2 to 3 times worse than horizontal in GPS measuring (Barnes, 2003, 2004, 2005).

In recent years, an alternative geodetic method with the use of robot total station or robot tachymeter (RTS) has been developed. A robot total station (RTS) is a new generation of geodetic instruments which automatically measure the length change, horizontal angle change and vertical angle change in motion. The method was successfully used in many measurements of semi-static (Koo, 2013) and dynamic displacements of size class of few centimetres (Psimoulis, 2012, 2013; Marendić, 2014a, 2016). Harder task for robot total stations is the measuring of dynamic parameters of short and stiffer objects. Higher natural frequencies, and lower amplitudes are characteristic for them. Current systematic experiments with RTS and built-in software have shown the capability of measuring the oscillation even up to 20 Hz (Marendić, 2014b) and an amplitude of a few millimetres. Despite that, only a few experiments with a recording frequency of 5–7 Hz have been carried out (Psimoulis, 2007). The deficiency of measuring equipment of mentioned methods with sensors (accelerometers, GNSS antennas) or special prisms (robot total station) is the need to install it on the observed structure.

In the works (Radovanovic, 2001; Kopačik, 2006; Stemfhuber, 2008) projects and results of studying the possible use of Robotic Total Station – RTS in monitoring the prism in motion are described. Authors primarily describe the deficiency of non-synchronicity of the functioning of the sensors for length and direction measuring instruments, which leads us to the systematic influence in determining the coordinates of the prism's position. In the works (Garget, 2005; Ceryova, 2006; Ehrhard, 2015), robotized total stations of different manufacturers to determine the prism's position which is moving on circular arcs are tested. In the work (Gikas, 2006), RTS at measuring the high-frequency displacements in a horizontal direction is tested. In the work (Coser, 2003), RTS at measuring the dynamic displacements of the bridge is tested; also, the possibilities and disadvantages of the use of RTS for this kind of measurements are provided. The biggest disadvantage of measuring instruments is a slow performance of measurements. In the work (Lekidis, 2005), the comparisons of dynamic parameters of the bridge, determined with GPS, RTS and accelerometers are introduced.

Among more interesting studies of the use of non-contact geodetic methods to measure the dynamic response of a structure in the last few decades next can be mentioned:

- Wilford Suspension Bridge (Great Britain), measured in 2002 (Coser, 2003).
- Rio Pelotas Bridge (Brazil), measured in 2006 (Palazzo, 2006).
- Gorgopotamos Bridge (Greece), measured in 2012 (Psimoulis, 2013).
- Sava River Bridge (Croatia), measured in 2016 (Marendić, 2016).

2 MATHEMATICAL PROBLEM

Many studies mentioned above have shown the adequacy of geodetic instruments in measuring dynamic displacement of structure, exposed to dynamic loads. Mentioned techniques are especially appropriate in oscillations with a frequency lower than 1 Hz and amplitude of up to 10 mm, which is characteristic

for bigger flexible structures such as bridges or high buildings. In stiffer structures with higher oscillation frequencies a noise appears while observing dynamic displacement with geodetic methods, which affects the accuracy of certain characteristic values of measurements. Measurements in the most of scientific and engineer fields are characterized by periodical signals; their periodicity is determined on a basis of a spectral analysis. The Fourier Transform is the most used technique for spectral analysis, which is also used for continuous and discrete signals. The main condition of the Fourier Transform is the condition of a constant time interval of measuring registration (registration of measurements in equal time intervals). In practice, we encounter the measuring data at processing geodetic measured data which are obtained at incorrect time intervals of measuring. The mentioned influence occurs at the carrying out of maximal permitted high-frequent measuring although the process of measuring is automated and has a foreseen constant data registration. Except that, there are often obtained data of incorrect time intervals when we analyse a whole range of data which are obtained with various methods and instruments (multi-sensors) and have various measuring frequencies (Shultz, 1999; Kircher, 2002). The key disadvantage of signals, obtained with geodetic methods such as RTS is that those signals are sampled unevenly. Incorrect images of a frequency spectre are thus returned by a spectral analysis with a method of fast Fourier Transform. Therefore, the main shortcoming of a Fourier Transform is non-compliance with time unevenness of sampling. It turns out this it is also a key reason to seek for a more appropriate method. Lomb-Scargle periodogram is a classic method for assessing frequency spectre and periodicity of evenly and unevenly sampled optional oscillations. The method is based on a principle of the smallest squares which connects data into sinusoids. In comparison to classic algorithms, first, the time lag τ which separates sinus and cosine forms of undulation is determined. The next equations describe time lag and an algorithm of periodogram (Press, 1988):

$$\tan 2\omega\tau = \frac{\sum_{j=1}^N \sin 2\omega\tau_j}{\sum_{j=1}^N \cos 2\omega\tau_j} \quad (1)$$

where ω means angular frequency, $P(\omega)$ refers to the function of the frequency.

$$P_x(\omega) = \frac{1}{2\sigma^2} \left(\frac{\left[\sum_{j=1}^N (X_j - \bar{X}) \cos \omega(t_j - \tau) \right]^2}{\sum_{j=1}^N \cos^2 \omega(t_j - \tau)} + \frac{\left[\sum_{j=1}^N (X_j - \bar{X}) \sin \omega(t_j - \tau) \right]^2}{\sum_{j=1}^N \sin^2 \omega(t_j - \tau)} \right), \quad (2)$$

where X_j is a value of displacement in time t_j for $j=1, 2, \dots, N$ and \bar{X} is a average value of displacements.

Variance σ^2 is calculated by the equation:

$$\sigma^2 = \frac{1}{N-1} \sum_{j=1}^N (X_j - \bar{X})^2 \quad (3)$$

$P(\omega)$ is without dimensions and expresses only spectral power. It can be achieved with normalization for periodogram to show periodicity. Maximums which express the proxy of an amplitude appear at frequencies which minimalize the sum of the squares of other values' fitting in a sinus oscillation of a time series. The level of importance p of each frequency is determined by equation (Psimoulis, 2012)

$$p = 1 - (1 - e^{-P(\omega)})^N \quad (4)$$

2.1 Algorithm to determine the average amplitude of oscillation

In those cases, the algorithm to determine the average amplitude of oscillation is used (Psimoulis, 2012). The algorithm works on a principle of filtering extreme values of oscillation. The algorithm as a filter is a function of oscillation frequency which eliminates errors because of the noise. The algorithm can be described in steps:

- Time series of changing coordinates (displacements in three directions) in a time interval of oscillation, as shown in Figure 1, present the main input data of the algorithm.

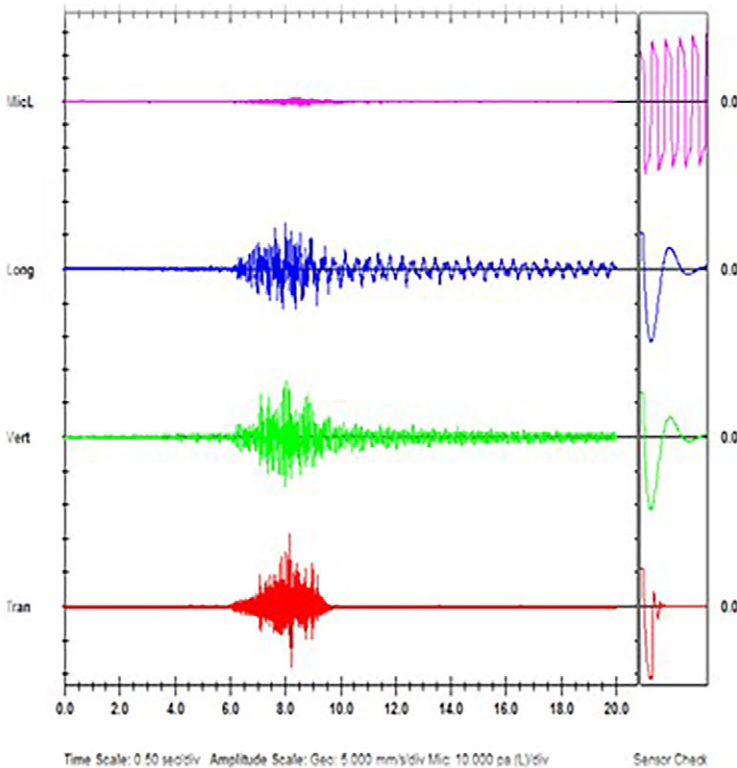


Figure 1: Measured displacements in three directions.

- In the case of availability of a sequence of intervals of no-motion, of oscillation and of no-motion, it is then checked whether the max amplitude of peaks in the time series of apparent displacements during the interval of oscillation exceeds those of no motion (i.e. reflecting noise). If not, the algorithm terminates (Psimoulis, 2012).
- The use of transmission of the extreme values filter for high-frequency components of an individual time series.
- Determine the spectral density of high-frequency component for each time series. The procedure is finished if there is no extreme in the oscillation interval which shows a dominant frequency f .
- Based on maximal dominant frequency f in oscillation interval, the parameter k_{RTS} is determined by the equation (5) as seen from Figure 2.

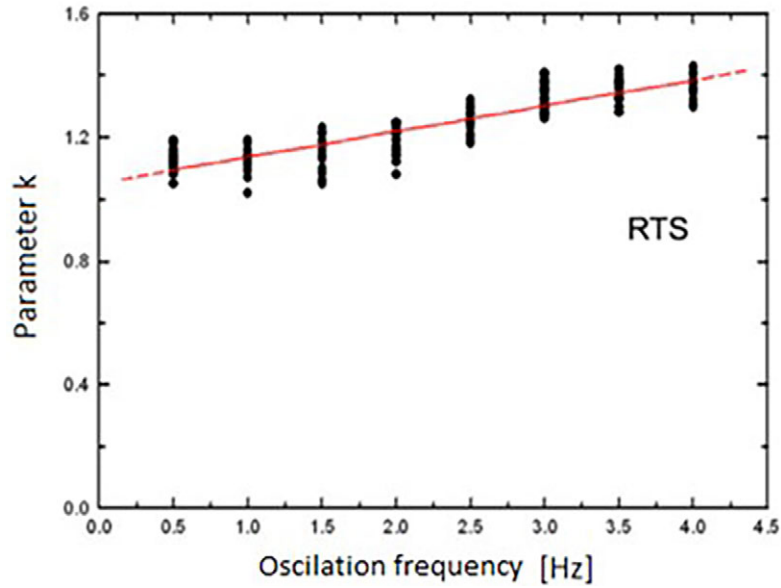


Figure 2: The dependence of the parameter k from the oscillation frequency (Psimoulis, 2012).

The data analysed derived from a large number of experiments based on a generator of linear oscillations which were recorded by both a dual frequency GPS receiver and a RTS (Psimoulis, 2012). The characteristics of each oscillation-experiment were predetermined, with the frequency ranging between of 0.5 and 4 Hz (limits imposed by the specifications of the oscillator used) with a step of 0.5 Hz and the amplitude between 5 and 30 mm with a step of 5 mm.; >150 experiments were made. The duration of each oscillation was approximately 60 s, corresponding to typical dynamic motions of engineering structures (for instance due to vehicles passing from a bridge or a seismic event. Recording by both instruments started and ended about 20 s before and after the oscillation, respectively. Hence each experiment lasted for about 100 s. The line in Figure 2 represents trend line of parameter k_{RTS} depending on oscillation frequency and is defined in equation 5.

$$k_{RTS} = 0.08f + 1.05 \tag{5}$$

- The middle oscillation amplitude is determined with the equation (6) based on the preliminary experiments, in which the parameter k is determined with the equation (5). It is necessary to introduce the parameter k into the procedure, since it turned out from the experimental cases, that there is a difference between the measured and actual shift with the GPS and RTS methods while increasing the frequency. Measured values of the shifts with the RTS method turn out to be lower than actual ones, therefore it is necessary to introduce a parameter k, based on which an appropriate filter is determined.
- Determining the adequacy of the filter affects the quality of obtained results, which optimally eliminates the extremes of lower amplitudes and enables for the average of the remaining extremes of higher amplitudes to converge to the real value of the oscillation amplitude. The deviation of the value of movements is proportional to the oscillation frequency. If the deviation is expressed with a

standard deviation, the amplitude A can be defined by the equation:

$$A = k\sigma, \quad k = k_{RTS}, k_{GPS}, k_{\dots} \tag{6}$$

Where σ is the spread in data and k a parameter to be defined from analysis of recordings of experiments of known characteristics (Psimoulis, 2012). This type of filter should be applicable to both GPS and RTS data, and the only difference should be the value of k (k_{GPS} , k_{RTS}), since the noise has a different effect on GPS and RTS data.

- The RTS data of time series are filtered with the use of the parameter above as a filter for the transmission of extreme values. Belonging standard deviations and average values of minimums and maximums \hat{a}^+ and \hat{a}^- are calculated by equations 9:
- If the method of data acquisition provides the quality assessment of the oscillation amplitude, the algorithm converges to the right solution and is successfully ended.

Let's take for example the sinus oscillation with the amplitude $a = 2\text{ cm}$, frequency $f = 5\text{ Hz}$, phase angle $\delta = \pi/2$ and belonging circle frequency $\omega = 2\pi f$, as shown in Figure 3.

The equation of selected oscillation in explicit form is:

$$x(t) = 2 \sin(10\pi t + 0.5\pi) \tag{7}$$

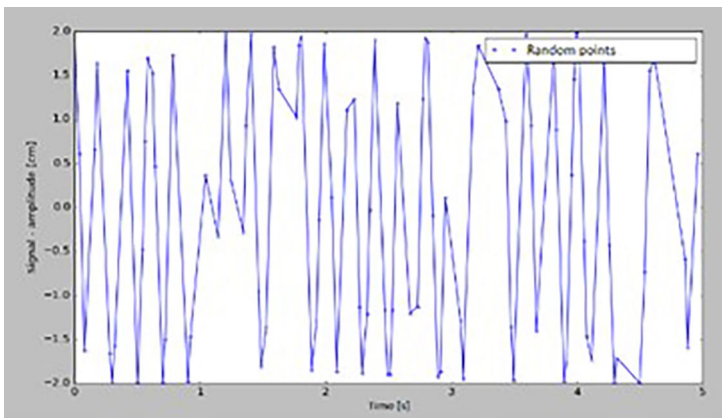


Figure 3: Simulated oscillation and display of uneven sampling rate, obtained by the program written in Python.

With the help of the built-in algorithm in Python, spectral analysis according to Lomb-Scargle method is performed. The effect of unevenness of sampling and frequency is shown in the form of noise on the graph of normalized Lomb-Scargle periodogram (left figure) and frequency (right figure) it can be seen from Figure 4.

The results of spectral analysis unambiguously show on harmonic oscillation with a frequency 5 Hz. Non-normalized Lomb-Scargle periodogram is used to know the frequency response. The diagram on the abscissa shows the frequency spectral power. It is necessary to normalize the periodogram to gain the amplitude data. In the case of non-normalized periodogram, the harmonic signal with the amplitude A in the frequency spectral density is treated as $A^2N/4$ for a sufficient number of samples N , which is determined based on the oscillation's nature. To get normalized Lomb-Scargle periodogram, the unnor-

malised value has to be multiplied by 4 and divided by the number of samples before calculating the root (Long, 2014). That way the data about the amplitude A is gained and with that, the correctness of the expressed spectral power can be confirmed.

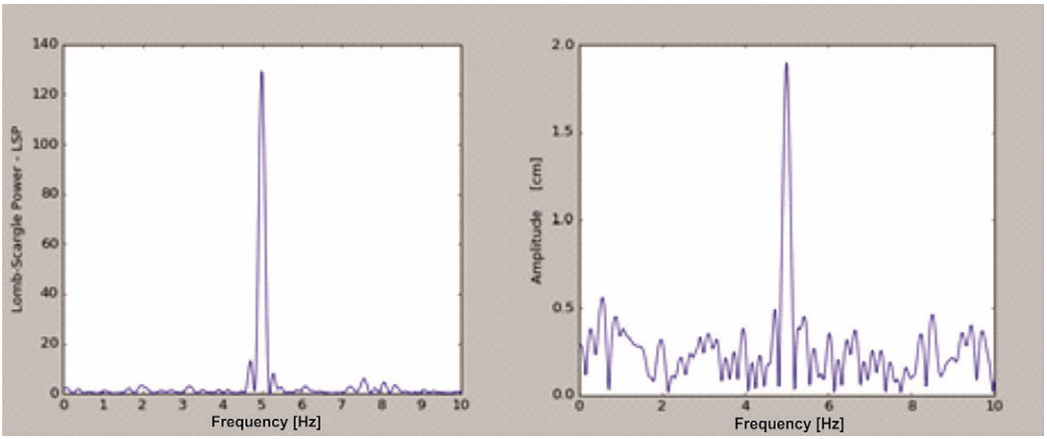


Figure 4: Lomb-Scargle periodogram (left), normalized Lomb-Scargle periodogram (right).

In this experiment, it can be seen what happens in the case if the sampling frequency is comparison with the original signal frequency is too low, as seen in Figure 5. In other words, to not fulfil the Nyquist condition of sampling. Figure 5 shows the result of spectral analysis at the too-low sampling frequency. In this case, we cannot talk about the dominant frequency nor the belonging amplitude.

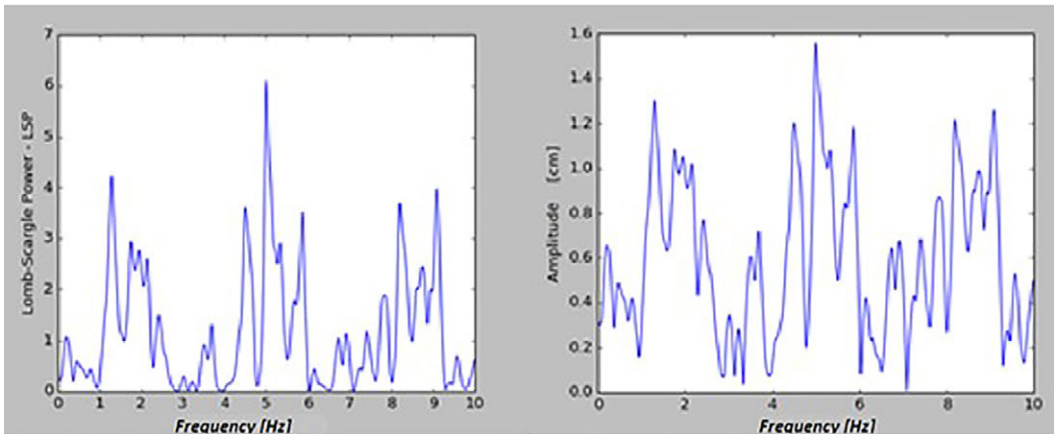


Figure 5: The example of spectral analysis of sampling with too-low frequency.

The computer algorithm can be optimized numerically as shown in Table 1. From the analysis above the response frequency data is obtained; it is key to determine the average amplitude with the help of the equation (9). From the oscillation input data, the standard deviation σ can be calculated by the equation:

$$\sigma = \sqrt{\frac{1}{N-1} \sum_{i=1}^N (X_j - \bar{X})^2} \tag{8}$$

The parameter $\theta = a/10 = 2/10 = 0.2$ is determined. The θ parameter represents the number of steps in the process. In our case, we divided the process into 10 steps. If we increase this number we get several steps and consequently a higher accuracy of the final value. With the help of equations (9, 10 in 11) for each value $\lambda = 1, 2, \dots, 10$, we calculate the values of qualities φ^\mp, \hat{a}^\mp in $\Delta\lambda^\mp$. The qualities are calculated numerically, and the result is provided in a table.

$$\hat{a}^+ = \frac{1}{n} \sum_{j=1}^N p_j^+ \rightarrow a \quad \hat{a}^- = \frac{1}{m} \sum_{j=1}^N -p_j^- \rightarrow -a \tag{9}$$

where n is number of high peaks and m is number of low peaks. With the incorporation of the parameter $\theta > 0, \theta \approx a/10$, the filter of high amplitudes' values φ^+ transmission is defined by the equation:

$$\varphi^+ = \lambda \cdot \theta \cdot \sigma \tag{10}$$

With the use of a filter for the displacements values u_i considering $\lambda = 1$ the time series is shaped in the form of:

$$r_p = \{u_1^+, u_2^+, \dots, u_p^+\}, \quad \text{where } p \leq n \text{ in } u_i^+ \geq \varphi^+ = \lambda \cdot \theta \cdot \sigma,$$

Which contains positive extremes above a certain threshold. Following is the determination of Δ_i^+ :

$$\Delta_i^+ = \alpha - \frac{\sum_{i=1}^p |u_i^+|}{p} = a - \hat{a}_\lambda^+, \tag{11}$$

Which represents the difference between the average value of positive extremes, determined by the filter and known amplitude a . The procedure is repeated with raising the value $\lambda = 1.2$. The aim is to reach $\Delta_i^+ \rightarrow 0$, when is $\lambda = \lambda^{*+}$. Consequently, the value of the parameter $k^+ = \lambda^{*+} \theta$ is achieved, which enables certain determination of the value α^* of the average amplitude's recorded oscillation at frequency f .

Table 1: Solution of numerical procedure in determining the average oscillation amplitude of computer simulated oscillation

λ	k^\mp	$\varphi^\mp [cm]$	$\hat{a}^\mp [cm]$	$\Delta\lambda^\mp [cm]$	$\hat{a}^\mp [cm]$	$\Delta\lambda^\mp [cm]$
1	0.2	0.277	1.32	0.679	-1.40	-0.596
2	0.4	0.554	1.45	0.543	-1.50	-0.496
3	0.6	0.831	1.56	0.432	-1.64	-0.356
4	0.8	1.108	1.70	0.290	-1.70	-0.296
5	1	1.386	1.81	0.182	-1.83	-0.167
6	1.2	1.663	1.88	0.112	-1.88	-0.118
7	1.4	1.940	1.98	0.023	-1.97	-0.029
8	1.6	2.217				
9	1.8	2.494				
10	2	2.772				

As described, the aim is to fulfil the condition of deviation $\Delta\lambda^\mp \rightarrow 0$. From the table 1 the red-marked values are read. The procedure is finished with step $\lambda = 7$, because in this step we reached an amplitude of 2 cm, which we read from the graph in Figure 3. Belonging amplitudes from the case have value $\hat{a}^+ = 1.98\text{ cm}$ and $\hat{a}^- = 1.97\text{ cm}$. Their average value is $\hat{a} = 1.975\text{ cm}$ and the influence against the actual

value only 0.0025 cm. The values of amplitudes are very similar in both directions because the influence ϵ and the influence of outside noise weren't considered in input data.

3 THE EXAMPLE OF DAMPED LAMELLA OSCILLATION

The aim is to measure the displacements of the structure which are the consequence of the imposed oscillation during a laboratory test. It's a typical example of damped Teflon lamella oscillation in the means of a console. It is referred to the damped oscillation when the oscillation energy is diminished because of resistance or friction with time. At real structure, that kind of oscillation is always dealt with. The structure which is evoked towards dynamic outside influence is resistant to oscillation and aims to equilibrium position because of the elasticity.

The equation of motion for the linear oscillation with damping for the discrete system is:

$$\frac{d^2 x}{dt^2} + 2\beta \frac{dx}{dt} + \omega_0^2 x = 0 \tag{12}$$

The solution of Eq (11) is:

$$x(t) = x_0 e^{-\beta t} \cos(\omega'_0 t + \delta) \tag{13}$$

The natural frequency remains the same:

$$\omega'_0 = \sqrt{\omega_0^2 - \beta^2} \tag{14}$$

The test is being observed simultaneously with two independent contact methods. The basic method for the lamella observation is the RTS with Leica TS 50, the second is photometry with camera (120 photos/sec). The lamella with dimensions 600 x 100 x 2 mm was attached to a stiff stand on one side and a mini prism was set on the lamella from the other side (Figure 6). The starting deviation from the equilibrium position of the load is caused by the deviation from the equilibrium position. Because the number of records is written faster, only the change of vertical angle is measured, meanwhile, when the length is measured in the equilibrium position. With the calculation of the value of angles and the given length in displacements, the changing amplitude of damped oscillation is determined. Figure 6 shows the position of the camera, measuring tape, mini prism and the end of the lamella.



Figure 6: The setting of the prism and measuring tape at the end of the lamella (Source: own) .

The test has been done with three repetitions with the aim to gain the best sample of damped oscillation possible. For further analysis, the one, shown in Figure 7, is chosen. With the help of data about RTS position and the prism, the size of the vertical displacements is being calculated. The first deviation to the extreme position is somehow bigger, which explains the starting influence on the lamella. The most interesting is especially the starting part of the oscillation (0 s – 25 s), where the amplitudes are the highest and the ratio between the noise and the signal is sufficient.

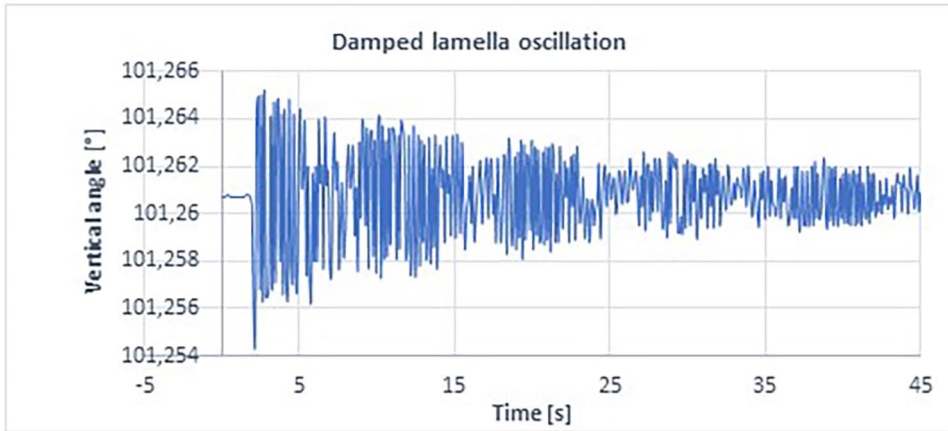


Figure 7: Damped lamella oscillation (the change of the vertical angle).

It is obvious that changes in the time of stagnation are very small. The amplitude can be determined from the data from the results of measured vertical angles (Figure 7) and knowing the distance between RTS and the prism. Considering that the distance to the prism is much bigger than the expected amplitude and that angle change is very small, the amplitude can be calculated with the help of triangles. If the angle φ is very small, it can be assured that triangles on Figure 8 are the right triangles and that $tg \varphi = \varphi$. The calculation is carried out numerically and the diagram of the amplitudes is made.

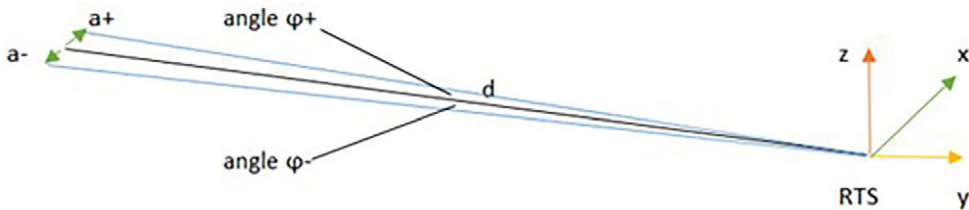


Figure 8: The sketch of assumptions for the calculation of the amplitude.

Where :

φ – angle

d – the distance between the prism and RTS (in case of experiment d = 4.5m)

a^+ , a^- – amplitude

φ^* , φ – measured angle

According to the specifications of most producers, modern RTS permit an accuracy of 0.5"–5" for angles and 2–10 mm for short-range robotic measurements. Analysis of various RTS using interferometry techniques revealed that for measurements up to 100–150 m, the accuracy of distance measurements is a fraction of an mm, while the accuracy in angles is relatively small for distances up to 10 m, but higher than the corresponding manufacturer specifications (0.5"–5") for distances >10 m (Martin, 2006). The combination of the noise of these measurements with the effect of the servo-mechanism, however, lead to much higher levels of noise for the observed polar coordinates (Cosser, 2003; Radovanović, 2001). On the other hand, because of the law of propagation of influences (Psimoulis, 2007), Cartesian coordinates computed from polar coordinates tend to be characterized by higher accuracies (or precision), usually between a fraction of an mm to 1–2 mm (Cook, 2006).

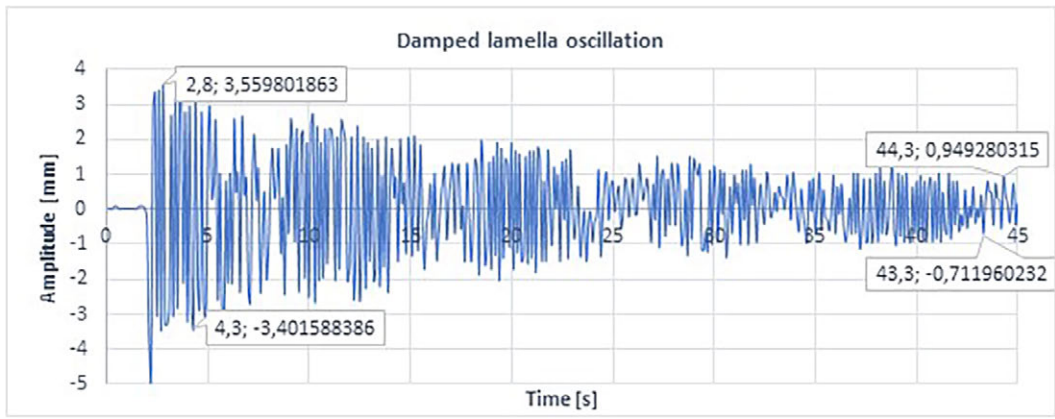


Figure 9: The amplitude of damped lamella oscillation.

The adequacy of the used method with the robot station can be compared with the photometry records. From the graph above the starting (maximal) deviations from the equilibrium position are read and compared to the results of the photometry, given in Table 2. From the record in slow motion three characteristic positions of the lamella are caught, as seen in Figure 10.

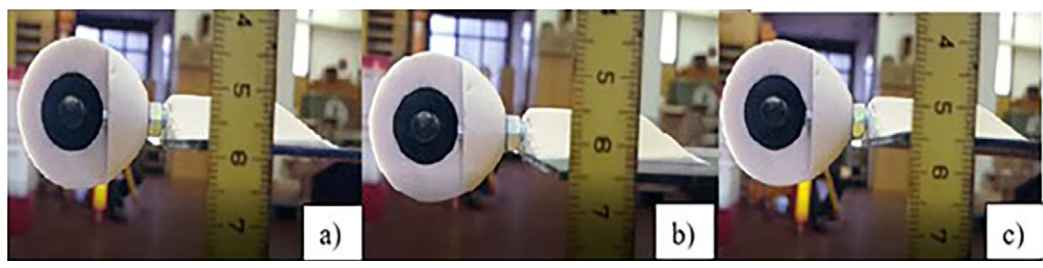


Figure 10: Three characteristic positions of the lamella: a) standing position, b) the first extreme position, c) the second extreme position (source: own).

Table 2: The comparison of calculated characteristic amplitudes' values

	Standing position	Extreme position below	Extreme position above
RTS	0 mm	-4.9 mm	3.5 mm
PHOTOMETRY	0 mm	5 mm	4 mm

In the next step, the function of the amplitude's changing over time and the intensity of damped system with the help of the damping factor for recorded data of damped oscillation can be determined. The amplitude of damped oscillation for the discrete system is in general written with the equation:

$$A(t) = A_0 e^{(-\beta t)}, \tag{15}$$

Where A_0 represents the starting deviation from the equilibrium position and β represents the damping constant. The boundary conditions from Figure 9 to determine the function for the present case are determined from the data, recorded with RTS, as shown in Table 3.

Table 3: Data to calculate the damping factor

	Time [s]	Amplitude [mm]	Damping factor β []
Side 1	2.8	3.56	0.0318
	44.3	0.95	
Side 2	4.3	-3.40	0.0402
	43.3	-0.71	

From the tabulated given data, the system of two equations with two x separately for the side 1 and 2 is set up. The solution of equation systems gives us the data about A_0 , which isn't interesting in this case and the data about damping factors β^* in β . Values of the damping factors should be equal but given the data, this is hard to achieve. The damping factor of the whole oscillation is expressed with the average value of both analytically determined and is $\beta = 0.036$. It is concluded, that differences of starting amplitudes among methods are relatively small and it is estimated that the RTS method is appropriate for observing the dynamic response of the size class of the amplitudes a few mm at the low level of the noise. On Figure 11 the mathematical function of the amplitude changes or the enveloping curve of the amplitudes of the addressed damped oscillation is also shown.

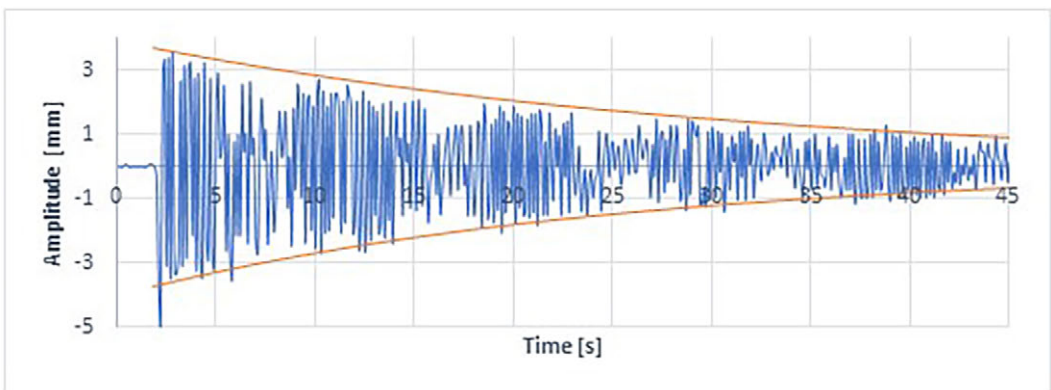


Figure 11: The function of the amplitude's change over time.

The same graph in Figure 11 shows the clipping effect of the RTS method assuming, that mathematical function presents the actual change of the amplitude. Despite that, the oscillation fits very good to the mathematical line of the amplitude's change.

4 CONCLUSION

The results of r experiments' studies and the experiment which was carried out on an actual structure, show the adequacy of used method RTS. In the test, the frequency spectral density from 1 Hz to 5 Hz and amplitudes from 0.1 mm to 5 mm was contained. At those ranges of frequencies and amplitudes, the geodetic methods proved out to be weaker. At performing the experiment in the laboratory, the RTS method proved to be an appropriate technique for recording damped oscillation with an amplitude less than a cm. This was shown with the comparison of the results, gained with the alternative method of photometry. The analysis of signals with the FFT and Lomb-Scargle methods proved as an amazing tool for presenting the oscillation frequency information. Although the FFT method doesn't consider the unevenness of the signal sampling, it turned out to be adequate for determining frequency spectre with an acceptable accuracy. The use of FFT method is possible because of quite even sampling of the RTS system. Higher accuracy is provided by the Lomb-Scargle method. The results of dynamic responses' measurements with RTS method show the progress of geodetic methods in identifying the structures' state in the sense of response on a dynamic load. There is still the problematics of sampling, which is a limit for geodetic methods in terms of accuracy and evenness in sampling. Geodetic methods cannot yet perform such big and evenly sampling as other physical methods in identifying dynamic characteristics of the structures.. For accurate analysis, it is necessary to incorporate alternative methods along with geodetic methods. In any case, non-contact geodetic methods are a fast, achievable and useful tool in construction, which enables the assessment of objects' dynamic characteristics while building and in periodical reviews of the state of building structures in their lifetime.

References:

Barnes, J., Rizos, C., Wang, J., Meng, X., Dodson, A. H., Roberts, G. W. (2003). The monitoring of bridge movements using GPS and pseudolites. In The 11th International Symposium On Deformation Measurements, Santorini, Greece, 25–28 May (pp. 563–572).

Barnes, J., Rizos, C., Kanli, M., Small, D., Voigt, G., Gambale, N., Lamance, J. (2004). Structural deformation monitoring using Locata. In The 1st FIG Int. Symposium on Engineering Surveys for Construction Works & Structural Engineering, Nottingham, U.K.

Barnes, J., Rizos, C., Lee, H. K., Roberts, G. W., Meng, X., Cosser, E., Dodson, A. H. (2005). The integration of GPS and pseudolites for bridge monitoring. In F. Sanso (ed.), *A Window on the Future of Geodesy*. IAG Symposium, 128, Springer-Verlag, pp. 83–88. DOI: https://doi.org/10.1007/3-540-27432-4_15

Ceryova, I., Kubanka, P., Kopačik, A., Kyrinovič, P. (2006). Dynamic Tests of Robot Stations. In International Congress, Washington, D.C. USA.

Cook D. (2006). Robotic total stations and remote data capture. Challenges in construction. *Geotechnical News*, 24, 42–5.

Cosser, E., Roberts, G. W., Dodson, A. H., Meng, X. (2003). Bridge monitoring, *Civil Engineering Surveyor, GIS/GPS Supplement*.

DeLoach, S.R. (1989). Continuous deformation monitoring with GPS. *Journal of Surveying Engineering*, 115 (1), 93–110. DOI: [https://doi.org/10.1061/\(asce\)0733-9453\(1989\)115:1\(93\)](https://doi.org/10.1061/(asce)0733-9453(1989)115:1(93))

Ehrhart, M., Lienhart, W. (2015). Development and evaluation of a long range image-based monitoring system for civil engineering structures. In *Proceeding SPIE*, 94370K–94370K–13. DOI: <https://doi.org/10.1117/12.2084221>

Garget, D. (2005). Testing of Robotic total Stations for Dynamic tracking. Doctoral Dissertation. University of Southern Queensland, Faculty of Engineering and Surveying.

Gikas, V., Daskalakis, S. (2006). Full scale validation of tracking total stations using a long stroke electrodynamic shaker. In The XXIII FIG congress shaping the change, Munich, October 8–13, 2006.

Kircher, J. (2002). Evolutionary speed limits inferred from the fossil record. *Nature*, 415, 65–68. DOI: <https://doi.org/10.1038/415065a>

Kogoj, D., Stopar, B. (2001). *Geodetska izmera [Geodetic measurements]*. Ljubljana: Slovenian Chamber of Engineers and University of Ljubljana, pp. 18–19.

Koo, K. Y., Brownjohn, J. M. W., List, D. I., Cole, R. (2013). Structural health monitoring of the Tamar suspension bridge. *Structural Control and Health Monitoring*, 20 (4), 609–625. DOI: <https://doi.org/10.1002/stc.1481>

Kopačik, A., Kyrinovič, P., Kadlecikova, V. (2006). Laboratory tests of robot stations. In *The Proceedings of FIG working week*, Cairo, April 16–20, 2005.

Lekidis, V., Tsakiri, M., Makra, K., Karakostas, C., Klimis, N., Sous, I. (2005). Evaluation of dynamic response and local soil effects of the Evripos cablestayed bridge using multi-sensor monitoring system. *Engineering Geology*, 79 (1–2), 43–59. DOI: <https://doi.org/10.1016/j.enggeo.2004.10.015>

Li, X. (2004a). Integration of GPS, accelerometers and optical fibre sensors for structural deformation monitoring, 17th Int. Tech. In *The Meeting of the Satellite Division of the U.S. Institute of Navigation*, Long Beach, California, (pp. 211–224).

Li, X., Ge, L., Tamura, Y., Yoshida, A., Rizos, C., Peng, G.D. (2004b). Seismic response of a tower as measured by an integrated RTK-GPS system. In *The 1st FIG International Symposium on Engineering Surveys for Construction Works & Structural Eng.*, Nottingham, U.K.

Li, X., Peng, G. D., Rizos, C., Ge, L., Tamura, Y., Yoshida, A. (2003). Integration of GPS, accelerometers and optical fibre sensors for structural deformation monitoring. In *The International Symposium on GPS/GNSS*, Tokyo, Japan (pp. 617–624).

Li, X., Rizos, C., Ge, L., Ambikairajah, E. (2005). 3D analysis of structural response monitored using integrated GPS and accelerometer system. In *The International Symposium on GPS/GNSS*, Hong Kong.

Li, X., Rizos, C., Ge, L., Ambikairajah, E., Tamura, Y., Yoshida, A. (2006). Building monitors: The complementary characteristics of GPS and accelerometer for monitoring structural deformation. *Inside GNSS*, 1 (2), 48–55.

Long, J. (2014). Recovering Signals from Unevenly Sampled Data. <http://josephlong.com/writing/recovering-signals-from-unevenly-sampled-data>.

Marendić, A., Paar, R., Duvnjak, I., Buterin, A. (2014). Determination of Dynamic Displacements of the Roof of Sports Hall Arena Zagreb. *Geodetski list*, 13–20.

Marendić, A. (2016). Monitoring of oscillations and frequency analysis of the railway bridge “Sava” using robotic total station. In *The Proceedings of 3rd Joint International Symposium on Deformation Monitoring (JISDM)* (pp. 1–8).

Marendić, A., Kapović, Z., Paar, R. (2014). Mogućnosti geodetskih instrumenata u određivanju dinamičkih pomaka građevina [Using the geodetic instruments to determine dynamic response of structures]. *Geodetski list*, 1–13.

Martin, D., Gatta, G. (2006). Calibration of total stations instruments at the ESRF. In *The Proceedings of XXIII FIG congress shaping the change*, Munich, October 8–13, 2006.

Meng, X., Dodson, A.H., Roberts, G. W. (2007). Detecting bridge dynamics with GPS and triaxial accelerometers. *Engineering Structures*, 29 (11), 3178–3184. DOI: <https://doi.org/10.1016/j.engstruct.2007.03.012>

Palazzo, D., Friedmann, R., Nadal, C., Filho, M. S., Veiga, L., Faggion, P. (2006). Dynamic Monitoring of Structures Using a Robotic Total Station. In *The Proceedings of XXIII FIG Congress*, Munich, October 8–13, 2006.

Press, W. H., Teukolsky, S. A., Vetterling, W. T., Flannery, B. P. (1988). *Numerical recipes: The art of scientific computing*. Cambridge University Press. DOI: <https://doi.org/10.2307/1269484>

Psimoulis, P. A., Stiros, S. C. (2007). Measurement of deflections and of oscillation frequencies of engineering structures using Robotic Theodolites (RTS). *Engineering Structures*, 29 (12), 3312–3324. DOI: <https://doi.org/10.1016/j.engstruct.2007.09.006>

Psimoulis, P. A., Stiros, S. C. (2012). A supervised learning computer-based algorithm to derive the amplitude of oscillations of structures using noisy GPS and Robotic Theodolites (RTS) records. *Computers and Structures*, 337–348. DOI: <https://doi.org/10.1016/j.compstruc.2011.10.019>

Psimoulis, P. A., Stiros, S. C. (2013). Measuring deflections of a short-span, railway bridge using a Robotic Total Station. *Journal of Bridge engineering*, 18 (2), 182–185. DOI: [https://doi.org/10.1061/\(asce\)be.1943-5592.0000334](https://doi.org/10.1061/(asce)be.1943-5592.0000334)

- Radovanovic, R. S., Teskey, W. F. (2001). Dynamic monitoring of deforming structures: GPS versus robotic tacheometry systems. In The Proceedings of 10th FIG symposium on deformation measurements. Orange, California.
- Roberts, G. W., Dodson, A., Ashkenazi, V. (1999). Twist and deflect, monitoring motion of the Humber Bridge, GPS World, 24–28.
- Roberts, G. W., Meng, X., Dodson, A. H. (2001). The Use of kinematic GPS and triaxial accelerometers to monitor the deflections of large bridges In The 10th FIG International Symposium on Deformation Measurements, Orange, California (pp. 19–22).
- Roberts, G. W., Cosser, E., Meng, X., Dodson, A. H. (2004). Monitoring the deflections of suspension bridges using 100 Hz GPS receivers. In The 17th International Technical Meeting of the Satellite Division of the U.S. Institute of Navigation, Long Beach, California, September 21–24, 2004.
- Roberts, G. W., Dodson, A. H., Brown, C. J., Karuna, R., Evans, E. (2000). Monitoring the height deflections of the Humber Bridge by GPS, GLONASS and finite element modelling. In Schwarz (ed.), Geodesy beyond 2000. IAG Symposia, Vol. 121. Berlin: Springer-Verlag (pp. 355–360). DOI: https://doi.org/10.1007/978-3-642-59742-8_58
- Rüeger, J. M. (2006). Overview of geodetic deformation measurements of Dams. Australian National Committee on Large Dams, Annual Congress of the Australian National Committee on Large Dams (ANCOLD), Sydney, Australia.
- Schulz, M., Statterger, K. (1999). Spectrum: spectral analysis of unevenly spaced paleoclimatic time series. Computer Geoscience, 23 (9), 929–945. DOI: [https://doi.org/10.1016/s0098-3004\(97\)00087-3](https://doi.org/10.1016/s0098-3004(97)00087-3)
- Stempfhuber, W. (2008). The Integration of Kinematic Measuring Sensors for Precision Farming. In The Proceedings of the 3rd International Symposium on Mobile Mapping Technology, Cairo.



Kovačič B., Motoh T. (2019). The possibility of measuring the dynamic response of structures using non-contact geodetic method. Geodetski vestnik, 63 (1), 57–72. DOI: <https://doi.org/10.15292/geodetski-vestnik.2019.01.57-72>

Assoc. Prof. Boštjan Kovačič, Ph.D.

University of Maribor, Faculty of Civil Engineering,
Transportation Engineering and Architecture
Smetanova 17, SI-2000 Maribor, Slovenia
e-mail: bostjan.kovacic@um.si

Tomaž Motoh, M.Sc. of Civil Eng.

Q Techna, Inštitut za zagotavljanje in kvaliteto kontrole
Cvetkova ulica 27, SI-1000 Ljubljana, Slovenia
e-mail: tomaz.motoh@gmail.com